Published in final edited form as:
Exp Neurol. 2012 January ; 233(1): 163–171. doi:10.1016/j.expneurol.2011.09.020.

Absence of SOD1 leads to oxidative stress in peripheral nerve and causes a progressive distal motor axonopathy

Lindsey R. Fischer[a], **Yingjie Li**[a], **Seneshaw A. Asress**[a], **Dean P. Jones**[b], and **Jonathan D. Glass**[a,c]

[a]Department of Neurology, Emory University School of Medicine, Atlanta, Georgia 30322 USA

[b]Department of Medicine, Emory University School of Medicine, Atlanta, Georgia 30322 USA

[c]Department of Pathology & Laboratory Medicine, Emory University School of Medicine, Atlanta, Georgia 30322 USA

Abstract

Oxidative stress is commonly implicated in the pathogenesis of motor neuron disease. However, the cause and effect relationship between oxidative stress and motor neuron degeneration is poorly defined. We recently identified denervation at the neuromuscular junction in mice lacking the antioxidant enzyme, Cu, Zn-superoxide dismutase (SOD1) (Fischer et al., 2011). These mice show a phenotype of progressive muscle atrophy and weakness in the setting of chronic oxidative stress. Here, we investigated further the extent of motor neuron pathology in this model, and the relationship between motor pathology and oxidative stress. We report preferential denervation of fast-twitch muscles beginning between 1 and 4 months of age, with relative sparing of slow-twitch muscle. Motor axon terminals in affected muscles show widespread sprouting and formation of large axonal swellings. We confirmed, as was previously reported, that spinal motor neurons and motor and sensory nerve roots in these mice are preserved, even out to 18 months of age. We also found preservation of distal sensory fibers in the epidermis, illustrating the specificity of pathology in this model for distal motor axons. Using HPLC measurement of the glutathione redox potential, we quantified oxidative stress in peripheral nerve and muscle at the onset of denervation. SOD1 knockout tibial nerve, but not gastrocnemius muscle, showed significant oxidation of the glutathione pool, suggesting that axonal degeneration is a consequence of impaired redox homeostasis in peripheral nerve. We conclude that the SOD1 knockout mouse is a model of oxidative stress-mediated motor axonopathy. Pathology in this model primarily affects motor axon terminals at the neuromuscular junction, demonstrating the vulnerability of this synapse to oxidative injury.

Address correspondence to: Jonathan D. Glass, MD, Emory Center for Neurodegenerative Disease, Whitehead Biomedical Research Building, 615 Michael Street, 5th Floor, Mailstop 1941007001, Atlanta, GA 30322, Phone: 404 727-3275/Fax: 404 727-3728/ jglas03@emory.edu.

Keywords

SOD1; axon; neuromuscular junction; oxidative stress; motor neuron; ALS

Introduction

Oxidative stress is commonly implicated in the pathogenesis of motor neuron disease. Markers of oxidative damage are increased in human amyotrophic lateral sclerosis (ALS), both familial and sporadic (reviewed in Barber et al., 2006). Attenuating oxidative stress confers robust survival benefits in mouse models of this disease, suggesting a role for oxidative stress in promoting disease progression (Crow et al., 2005; Marden et al., 2007; Harraz et al., 2008). However, clinical trails of antioxidant therapies have been unsuccessful to date (Louwerse et al., 1995; Desnuelle et al., 2001; Graf et al., 2005). A more precise understanding of the effect of oxidative stress on the neuromuscular system is needed.

Mutations in the antioxidant enzyme Cu, Zn-superoxide dismutase (SOD1) have long been known to cause familial ALS, and transgenic mice that overexpress mutant human SOD1 are the most widely studied model of ALS. Toxicity of mutant SOD1 is attributed to multiple gains of function, including a propensity to misfold, to accumulate in mitochondria, and to engage in aberrant redox chemistry (reviewed in Boillée et al., 2006; Rothstein, 2009). There is a well-established increase in oxidative stress in the SOD1 mutant model, but the multifactorial nature of disease makes this an unsuitable model in which to isolate the specific role of oxidative stress on motor neurons.

The SOD1 knockout mouse (*Sod1*−/−) is a model of chronic oxidative stress due to systemic deletion of SOD1. These animals were initially reported to lack a motor phenotype when studied out to 6 months of age (Reaume et al., 1996), a conclusion that remains widespread in the motor neuron disease literature. However, longer-term studies show age-related muscle atrophy, weakness, and accelerated senescence, with approximately 30% reduction in lifespan (Flood et al., 1999; Elchuri et al., 2005; Muller et al., 2006). Weakness in *Sod1*−/− mice, seen on grip strength (Fischer et al., 2011) and Rotarod testing (Muller et al., 2006), does not correlate with proximal motor pathology, since no spinal motor neuron or ventral root motor axon loss is observed, even at advanced ages (Flood et al., 1999; Shefner et al., 1999). However, muscle fiber atrophy can be appreciated in cross sections of hind limb muscle by 6 months of age (Flood et al., 1999), and we recently demonstrated denervation at the neuromuscular junction, beginning between 1 and 4 months of age (Fischer et al., 2011).

In this study, we investigated the spatial and temporal features of neuropathology in the *Sod1*−/− mouse, compared to the level of oxidative stress in peripheral nerve and muscle. We found preferential denervation of fast twitch muscle, accompanied by widespread sprouting and formation of large, neurofilament-rich axon swellings. Distal motor axons were preferentially affected, as we saw no degeneration of proximal motor axons or spinal motor neurons. Distal sensory axons were also spared. Oxidation of the glutathione pool in peripheral nerve, but not muscle, correlated with the onset of denervation, consistent with a relative impairment of redox homeostasis within peripheral nerve. Axon outgrowth in

Sod1−/− primary motor neurons was improved by treatment with the glutathione precursor, N-acetylcysteine, suggesting that the redox state in motor axons is important for axon maintenance. We conclude that chronic oxidative stress in the SOD1 knockout mouse causes a progressive motor axonopathy, with features reminiscent of distal axonal degeneration seen in other models of motor neuron disease.

Materials and Methods

Animals

The Emory University Institutional Animal Care and Use Committee approved all animal procedures in this study. *Sod1*−/− mice, generated by Huang and colleagues (Huang et al., 1997), were obtained from Marie Csete (Emory University) (Muller et al., 2006). *Sod1*−/− mice were crossed with *thy1-YFP16* mice as previously described (Fischer et al., 2011) to generate *Sod1*−/− mice and littermate controls expressing YFP in all peripheral nerve axons.

NMJ morphology

Neuromuscular junctions in medial gastrocnemius, tibialis anterior, and soleus muscles were assessed as previously described with minor modifications (Fischer et al., 2004). 35 μm frozen sections were cut longitudinally through the entire muscle, and every fourth section was examined. Nicotinic acetylcholine receptors at the motor endplate were labeled with Alexa Fluor 555-conjugated α-bungarotoxin (Invitrogen). Motor axon terminals were identified by YFP fluorescence. Innervated, intermediate, and denervated endplates were defined by complete, partial, or absent overlap between nerve terminal and endplate, respectively. Ultraterminal sprouts were defined as processes originating from the endplate region that could be clearly distinguished from the incoming axon (Aigner et al., 1995; Tam and Gordon, 2003).

Epidermal nerve fibers

The density of nerve fibers in the second plantar footpad was determined by the method of Hsieh and colleagues (Hsieh et al., 2000). 30 μm frozen sections were cut perpendicular to the skin surface along the entire footpad. Every fourth section was stained with PGP 9.5 (1:600, UltraClone), followed by FITC goat anti-rabbit secondary (1:100). Intra-epidermal nerve fibers were counted by an investigator who was blinded to genotype. Results were expressed as the number fibers per millimeter of epidermis, as determined using ImageJ software (http://rsb.info.nih.gov/ij/).

Immunohistochemistry

8 μm paraffin sections of lumbar spinal cord were probed by standard methods with the following antibodies: GFAP for astrocytes (1:1000, DAKO), Iba1 for microglia (1:1000, Wako), SMI-31 for phosphorylated neurofilament (NF-H/NF-M, 1:500, Sternberger Monoclonals), ubiquitin (1:400, DAKO), and TDP-43 (1:1000, Proteintech).

Redox potential

Molar concentrations of glutathione (GSH) and glutathione disulfide (GSSG) in tibial nerve and gastrocnemius were determined by HPLC (Jones, 2002; Jones et al., 2004). Fresh tissues were rapidly dissected and homogenized in 5% (w/v) perchloric acid containing 0.2 M boric acid and 10 μM γ-EE (internal standard). Thiols were derivitized with iodoacetic acid and dansyl chloride to form *S*-carboxymethyl, *N*-dansyl derivatives for HPLC analysis with fluorescent detection. Quantification was obtained by integration relative to the internal standard and normalized to protein concentration as measured by the DC Protein Assay (Bio-Rad). The redox potential E_h (in mV) was calculated using the Nernst equation:

$$E_h = E_0 + (2.303RT/nF) * \log([\mathrm{GSSG}]/[\mathrm{GSH}]^2.$$

Confocal imaging

Neuromuscular junction images were captured on a Zeiss LSM 510 NLO META system, coupled to a Zeiss Axiovert 100M inverted microscope. Z-stacks were obtained with a Plan-Neofluar 40x (NA 1.3) oil objective with optical slice thickness of 1 μm. Z-stacks were compressed and images exported using LSM Image Examiner software (Zeiss).

Statistical analysis

Results are expressed as mean ± standard deviation unless otherwise noted. Comparisons among genotypes were made by one-way ANOVA followed by Tukey post-hoc analysis ($\alpha = 0.05$) using Prism software (GraphPad).

Results

Fiber-type specificity of denervation in *Sod1−/−* mice

We recently reported that *Sod1−/−* mice show progressive denervation of tibialis anterior, a hind limb muscle composed primarily of fast twitch (type II) muscle fibers (Fischer et al., 2011). However, loss of muscle mass in these animals is not uniform. Fast twitch muscles of the hind limbs exhibit greater atrophy over time than slow twitch (Muller et al., 2006).

To determine whether susceptibility to denervation in *Sod1−/−* mice differs by muscle fiber type, we compared neuromuscular junction innervation from 1 to 18 months of age in tibialis anterior and medial gastrocnemius, both fast twitch muscles, to soleus muscle, which has a higher proportion of slow-twitch (type I) fibers (Wigston and English, 1992; Hegedus et al., 2007). Preliminary results showed an identical rate of denervation in tibialis anterior and medial gastrocnemius (Fig. 1A), so full morphologic comparison was limited to tibialis anterior and soleus, while gastrocnemius was reserved for oxidative stress studies as described below.

The tibialis anterior was fully innervated at one month of age (Fig. 1B), but by four months significant denervation had taken place. Only 70% of endplates in *Sod1−/−* tibialis anterior were innervated at four months, compared to >95% innervation in *Sod1+/+* and *Sod1+/−* mice ($p<0.001$). By 18 months, only 34% of endplates were still innervated ($p<0.001$ vs. *Sod1+/+*). In contrast, no significant denervation was seen in soleus until 12 months of age (Fig. 1C). Even at 18 months, 79% of endplates remained fully innervated in *Sod1−/−* mice

(p<0.05 vs. *Sod1*+/+). This same pattern of susceptibility to denervation is seen in mice overexpressing mutant SOD1 (Pun et al., 2006; Hegedus et al., 2007), although the underlying mechanism is unclear.

Morphologic abnormalities in motor axon terminals

In addition to denervation, we observed morphologic abnormalities in distal motor axons of *Sod1*−/− mice that were prominent in tibialis anterior and gastrocnemius by 4 months of age, with later onset in soleus muscle (Fig. 2). These include axonal and ultraterminal sprouting (Fig. 2A–D) and terminal axon swellings (Fig. 2E–F).

Ultraterminal sprouts, defined as axon processes originating from the endplate region that could be clearly distinguished from the incoming axon (Aigner et al., 1995; Tam and Gordon, 2003), were quantified as a percent of total endplates. By 1 month of age, 5% of terminals in *Sod1*−/− tibialis anterior had ultraterminal sprouts, compared to <1% in *Sod1*+/+ *and Sod1*+/− (p<0.001) (Fig. 2C). This was surprising given that we saw no evidence of denervation at this time point. In soleus, we found a similar trend (Fig. 2D). At 4 months, long before the onset of denervation, 6% of endplates had ultraterminal sprouts (p<0.01 vs. *Sod1*+/+). The extent of sprouting was more severe in tibialis anterior than in soleus at every time point, peaking at 16% in tibialis anterior at 12 months, and 9% in soleus at 18 months.

In addition to sprouting, we also observed large terminal axon swellings in tibialis anterior (Fig. 2E), and to a lesser extent in soleus. These swellings most commonly involved motor axon terminals, but smaller varicosities were also seen along the intramuscular nerve fibers in *Sod1*−/− mice, which were rare in control animals. The terminal swellings showed dense accumulation of phosphorylated neurofilament, which is also seen in other mouse models of motor neuropathy (Murray et al., 2008), and in Wallerian degeneration (Glass and Griffin, 1991).

Lack of proximal pathology

Previous studies have failed to identify pathology affecting proximal motor structures in *Sod1*−/− mice. No difference was seen in the number or size of *Sod1*−/− lumbar motor neurons at 6, 9, or 17 months (Shefner et al., 1999). Additionally, no difference was seen in the number of myelinated axons in L3 ventral and dorsal roots at 6 or 19 months, although ~10% decrease in axon diameter was noted at both ages (Flood et al., 1999).

We examined spinal cord and peripheral nerve from the same animals used for NMJ analysis, to confirm the absence of proximal pathology. Nissl-stained motor neurons in the ventral horn of lumbar spinal cord showed no evidence of motor neuron loss, vacuolation or chromatolysis at 4 or 18 months of age (Fig. 3A). Similarly, we found no degenerating axons in L4 ventral and dorsal roots, sciatic nerve, tibial nerve, and sural nerve in 18 month-old *Sod1*−/− mice (Fig. 3B and not shown).

To screen for more subtle evidence of pathology, we stained lumbar spinal cord from 4 and 18 month-old *Sod1*−/− and *Sod1*+/+ mice for common markers of neurodegeneration and gliosis (Fig. 3C). No accumulation of phosphorylated neurofilament was seen in motor

neurons or proximal axons at either time point. A mild increase in GFAP-positive astrocytes was seen in *Sod1*−/− mice at both 4 and 18 months of age, but no microgliosis was seen on Iba1 staining. Spinal cords were also probed for ubiquitin- and TDP-43-positive inclusions, which were absent. Nuclear TDP-43 localization within motor neurons appeared identical to controls at both time points. Thus, consistent with previous reports, we found no evidence to indicate proximal motor pathology in *Sod1*−/− mice, and saw little evidence of reactive changes in the lumbar spinal cord, even in 18 month-old animals.

Sparing of distal sensory fibers

Since motor pathology in *Sod1*−/− mice is restricted to the distal axon, we investigated whether distal sensory fibers are similarly affected. Epidermal nerve fibers of the plantar footpads are innervated by the sciatic nerve (Hsieh et al., 2000). Sensory axons course through a similar environment as motor axons innervating hind limb muscles and are of similar length. At 4 and 18 months of age, we assessed the density and morphology of epidermal nerve fibers (Fig. 4). No difference in fiber density between *Sod1*−/− mice and controls was seen. *Sod1*+/+ and *Sod1*+/− mice were identical at both time points, so were combined. A subtle increase in epidermal nerve fiber branching was seen in *Sod1*−/− mice at 18 months, but this would have been unlikely to affect quantification, as only those fibers entering the epidermis, not intra-epidermal branches, were counted. Our findings are consistent with behavioral data showing normal performance of 22 month-old *Sod1*−/− mice on a hot plate somatosensory test (Flood et al., 1999). The finding that distal sensory axons are spared in this model, in contrast to motor axons, suggests that motor axons may be inherently more sensitive to oxidative stress than sensory axons, or may be exposed to higher levels of oxidative stress *in vivo.*

Redox potential of peripheral nerve and muscle

To determine the contribution of oxidative stress in peripheral nerve and muscle to distal motor axon defects in *Sod1*−/− mice, we measured the steady-state redox potential of glutathione in tibial nerve and gastrocnemius muscle at 4 months of age. Our goal was to localize oxidative stress at the onset of motor pathology.

Glutathione, a major thiol antioxidant, is a principal redox buffer in cells and is routinely used as a representative indicator of the intracellular redox state (Schafer and Buettner, 2001; Jones, 2002; Jones et al., 2004). Here, reduced (GSH) and oxidized (GSSG) glutathione were measured by HPLC in homogenates of tibial nerve and gastrocnemius muscle from 4 month-old mice. The Nernst equation was then used to derive the GSH redox potential (E_h). Perturbations causing oxidation and/or depletion of the GSH pool are reflected by higher (more positive) values of E_h. To our knowledge, there are no published measurements of these values from peripheral nerve. E_h typically ranges from −230 to −260 mV in proliferating cells, −190 to −220 mV in differentiated cells, and −140 to −180 mV in apoptotic cells (Jones, 2006).

Measurements from tibial nerve at 4 months of age showed a redox potential of −215 mV in *Sod1*+/+ mice and −211 mV in *Sod1*+/− mice (Fig. 5A–C). *Sod1*−/− tibial nerve showed a significantly more oxidized redox potential at −195 mV ($p<0.001$), due to a decrease in GSH

and concomitant increase in GSSG. These measurements were taken from the proximal tibial nerve (above the level of the knee and the branch to the gastrocnemius). We also evaluated the distal tibial nerve (below the level of the knee) to determine if the redox potential varied along the course of the nerve (Supplemental Fig. 1). We found that even in wild type mice, the distal tibial nerve was at a more oxidized redox potential than the proximal tibial nerve (−215 mV proximal, −206 mV distal, $p<0.05$). This same trend was also seen in *Sod1*−/− mice (−195 mV proximal, −178 mV distal, $p>0.05$). Thus, there appears to be an oxidation of the GSH pool in distal vs. proximal tibial nerve, and *Sod1*−/− mice are shifted towards a more oxidized redox potential along the entire length of the nerve.

In contrast, the redox potential of *Sod1*−/− gastrocnemius, which is innervated by tibial nerve and shows significant denervation at 4 months, did not differ from controls (Fig. 5D–F). We also compared the redox potential of gastrocnemius, tibialis anterior, and soleus muscle, and found no difference that might explain the resistance of soleus to denervation (Supplemental Fig. 2). These data suggest that the development of axon pathology in *Sod1*−/− mice at 4 months correlates best with oxidative stress in peripheral nerve rather than muscle.

Antioxidant rescue of motor axon outgrowth

Primary motor neurons from *Sod1*−/− mice are short-lived and exhibit poor axon outgrowth (Fischer et al., 2011). To determine the effect of GSH replacement on axon outgrowth, *Sod1*−/− primary motor neurons were treated with the antioxidant N-acetylcysteine (NAC) (Fig. 6). NAC is hydrolyzed to cysteine inside cells, where it acts as a precursor for GSH synthesis. NAC also acts as a free radical scavenger and has GSH-independent effects on the cellular thiol/disulfide status (Jones et al., 1995; Schafer and Buettner, 2001; Jones et al., 2004).

When cultured in the absence of antioxidant supplements, *Sod1*−/− cells showed a marked reduction in axon outgrowth compared to controls (Fig. 6B). When NAC was added at the time of plating, a dose-dependent rescue of axon outgrowth was observed (Fig. 6C). Axons treated with the highest dose of NAC (5 mM) were indistinguishable from wild-type cells at 24 hours. This demonstrates that *Sod1*−/− motor axon outgrowth *in vitro* depends on the intrinsic level of oxidative stress.

Discussion

Distal axonal degeneration is an early event in motor neuron disease with important functional consequences— disrupting communication between a motor neuron and its target muscle. Axon protective therapies are needed, but the mechanism of axonal degeneration in motor neuron disease remains poorly understood. In this study, we illustrate the morphological and biochemical correlates of distal motor axonopathy in the *Sod1*−/− mouse, a model based on genetic deletion of a major antioxidant enzyme. This model provides proof of principle that loss of antioxidant protection is sufficient to cause a progressive distal motor axonopathy. Given the compelling evidence for oxidative stress in ALS (Barber et al., 2006), oxidative stress deserves increased attention as a mechanism that

may contribute to axonal degeneration in motor neuron disease. Determining the precise mechanism of oxidative injury to axons and exploring ways to block this effect may yield new strategies for axonal protection.

SOD1 is required for motor axon maintenance

Survival of motor axons is one of numerous roles for SOD1 that have been identified in SOD1 knockout models. Lack of SOD1 causes a 30% reduction in lifespan in mice, an increased risk of hepatocellular carcinoma (Elchuri et al., 2005), and numerous other age-related changes, including retinal degeneration (Hashizume et al., 2008), cochlear hair cell loss (McFadden et al., 1999), cataracts (Reddy et al., 2004), and vascular dysfunction (Didion et al., 2002). *Sod1*−/− neurons are also more vulnerable to cell death due to facial nerve axotomy (Reaume et al., 1996), ischemia (Kondo et al., 1997), and glutamate excitotoxicity (Schwartz et al., 1998).

The majority of intracellular superoxide is produced as a byproduct of mitochondrial electron transport along the inner mitochondrial membrane, and released both into the mitochondrial matrix (the site of SOD2 expression), and into the mitochondrial intermembrane space, where a fraction of SOD1 is normally found (Weisiger and Fridovich, 1973; Muller et al., 2004). Targeted replacement of SOD1 exclusively in the mitochondrial intermembrane space reverses the pathologic and phenotypic changes seen in *Sod1*−/− mice (Fischer et al., 2011), suggesting that the mechanism by which SOD1 protects motor axons is through regulation of mitochondrial superoxide levels. Moreover, it suggests that oxidative stress originating in mitochondria is an underlying cause of axonal degeneration in this model.

Susceptibility of the distal motor axon

An important question is why systemic deletion of SOD1 causes degeneration of only the distal-most portion of motor axons. This may reflect an intrinsic susceptibility of the distal motor axon to oxidative stress, increased oxidative stress in the environment surrounding the distal motor axon, or both. Technically, it is not feasible to measure the local GSH redox potential at the neuromuscular junction, so we assayed homogenates of tibial nerve and gastrocnemius muscle. We found that oxidative stress in peripheral nerve correlates best with the onset of denervation. Moreover, we were able to improve motor axon outgrowth in cultured neurons by treating with a GSH precursor, suggesting that the redox state in motor axons is important for axon maintenance. Flood and colleagues showed that replacement of SOD1 exclusively in neurons of *Sod1*−/− mice prevents muscle fiber atrophy and fiber type grouping (Flood et al., 1999), adding further support to the idea that oxidative stress within neurons causes axonal degeneration in this model. However, sensory and motor axons innervating the hind limbs course through the same environment *in vivo*, and we found that sensory fibers in *Sod1*−/− mice do not degenerate. A similar argument can be made for motor axons innervating slow twitch muscle fibers.

An alternative hypothesis is that vulnerable motor axon terminals are exposed to a greater degree of oxidative stress in the immediate environment. This hypothesis is attractive given the difference in susceptibility to denervation based on fiber type. Release of ROS during

muscle contraction is a well-described phenomenon (reviewed in Reid and Durham, 2002), and muscle mitochondria isolated from *Sod1−/−* mice show increased ROS release (Muller et al., 2007). Oxidative damage to proteins, lipids, and DNA in *Sod1−/−* muscle was previously shown to be increased by 5 months (Muller et al., 2006). However, we did not find an increase in the GSH redox potential in *Sod1−/−* gastrocnemius at 4 months of age, nor did we find a difference in the redox state between tibialis anterior, gastrocnemius, or soleus muscles that might explain differences in their innervation (not shown). The reason for the discrepancy between our results and those of Muller and colleagues is unclear, but may relate to the different methodologies used. The potential role of muscle as a source of ROS leading to axon damage remains to be clarified.

In this study, we took advantage of *Thy1-YFP16* mice, a powerful tool for examining NMJ morphology. However, a recent study suggested that data from these mice should be interpreted with caution (Comley et al., 2011). The authors showed that YFP expression causes upregulation of stress markers in the spinal cord, and increases neurofilament staining in distal motor axons at the neuromuscular junction in otherwise normal animals. However, they also reported that YFP expression slowed the rate of denervation in the *wasted* mouse, a model of dying-back axonopathy. Our initial observation of denervation in the SOD1 knockout mouse was made on PGP9.5-immunostained sections from non-YFP expressing mice (not shown). While we cannot exclude some contribution of YFP expression to changes in NMJ morphology in these mice, all of our comparisons were made using wild-type littermates that also expressed YFP. The axonal swelling and neurofilament accumulation we observed were markedly more severe in the *Sod1−/−* mice, and were more often seen at degenerating terminals. Finally, the rate of denervation we report here is consistent with the rate of electrophysiologic changes (Shefner et al., 1999) and muscle atrophy (Flood et al., 1999) reported in previous studies of non-YFP expressing animals, suggesting that YFP did not substantially alter the rate of denervation in this model.

Significance of premature sprouting

We were surprised to observe sprouting in *Sod1−/−* mice prior to the onset of denervation, rather than as a response to denervation that had already occurred. We examined neuromuscular junctions at 100 μm intervals throughout each muscle, so it is unlikely that we missed denervation significant enough to produce the sprouting observed. One exception was that *Sod1−/−* soleus showed a statistically significant difference in innervation at 1 month (6% in *Sod1−/−* versus 1% in *Sod1+/+*, $P<0.05$). This could have contributed to the sprouting we observed in soleus at 4 months. However, the statistical significance of this subtle change is most likely due to low variation between mice, and given that this apparent denervation resolved by 4 months, the biological significance is unclear. Still, we cannot exclude the possibility that sprouting in the soleus was caused by partial denervation.

There is evidence to suggest that oxidative stress may be sufficient to induce spontaneous sprouting. Oxidative stress has been postulated to inhibit vesicle release at the neuromuscular junction through oxidative damage to SNAP-25 (Giniatullin et al., 2006). This is analogous to the sprout-inducing mechanism of botulinum toxin (Blasi et al., 1993). Phosphorylation of GAP-43, which promotes spontaneous sprouting at the neuromuscular

junction *in vivo* (Aigner et al., 1995), is also controlled by a redox-sensitive mechanism (Gopalakrishna et al., 2008).

Although we saw widespread sprouting morphologically, previous electrophysiological analysis of *Sod1*−/− mice suggested that these mice have inadequate sprouting. Shefner and colleagues found a lack of increase in motor unit size in *Sod1*−/− mice to compensate for the ongoing loss of motor units (1999). This suggests that the sprouting we observed may not lead to the establishment of new functional synapses. There is evidence that chronic sprouting outside of the context of partial denervation may be detrimental. Subsets of transgenic mice expressing high levels of GAP-43, causing spontaneous sprouting in fully innervated muscles, went on to develop motor abnormalities (Aigner et al., 1995). Studies to manipulate sprouting in the *Sod1*−/− mouse are needed to explore whether this has an effect on the progression of denervation and motor symptoms.

Relevance to mutant SOD1-mediated ALS

Over 100 different SOD1 mutations have now been implicated in familial ALS, and overexpression of mutant human SOD1 in mice causes fatal motor neuron disease (reviewed in Rothstein, 2009). Compared to SOD1 mutant mice, the phenotype of *Sod1*−/− mice is milder, progresses more slowly, and never reaches full-blown paralysis. However, it seems unlikely to be a coincidence that both mutation and deletion of SOD1 cause motor deficits that share certain pathologic features, including (1) early involvement of distal motor axons, (2) preferential involvement of motor versus sensory fibers, (3) susceptibility of fast versus slow motor units, and (4) attempts at regenerative sprouting that are inadequate to compensate for progressive denervation over time.

The deleterious effects of mutant SOD1 are attributed to a toxic gain of function rather than a loss of function, since many of the mutant enzymes retain some degree of dismutase activity (Borchelt et al., 1994). Additionally, overexpression of mutant SOD1 in mice causes disease in a dose-dependent manner, despite super-normal levels of enzyme activity in affected tissues (Turner et al., 2003). Our current findings in *Sod1*−/− mice do not contradict the gain of function hypothesis for mutant SOD1 toxicity. Rather, they raise the question of whether oxidative stress associated with perturbations in SOD1 may cause motor axon pathology in both models. Numerous mechanisms have been proposed for how mutant SOD1 causes oxidative stress, including participation in aberrant redox reactions that generate rather than neutralize free radicals (reviewed in Barber et al., 2006). Mutant SOD1 also has a propensity to aggregate in mitochondria (Vijayvergiya et al., 2005), which has unknown consequences for local SOD1 activity and oxidative stress within distal axons. Thus, we propose that whether by loss or gain of function, oxidative stress associated with alterations in SOD1 is particularly detrimental to distal motor axons.

Supplementary Material

Refer to Web version on PubMed Central for supplementary material.

Acknowledgments

This work was supported by the Robert Packard Center for ALS Research and NIH T32 ES12870. We thank Marie Csete for providing *Sod1*−/− breeders and for helpful discussion, Bill Liang for assistance with HPLC, and Debbie Cooper for assistance with paraffin processing and TDP-43 staining.

References

Aigner L, Arber S, Kapfhammer JP, Laux T, Schneider C, Botteri F, Brenner HR, Caroni P. Overexpression of the neural growth-associated protein GAP-43 induces nerve sprouting in the adult nervous system of transgenic mice. Cell. 1995; 83:269–278. [PubMed: 7585944]

Barber S, Mead R, Shaw P. Oxidative stress in ALS: A mechanism of neurodegeneration and a therapeutic target. Biochimica et Biophysica Acta (BBA) - Molecular Basis of Disease. 2006; 1762:1051–1067.

Barber SC, Mead RJ, Shaw PJ. Oxidative stress in ALS: a mechanism of neurodegeneration and a therapeutic target. Biochim Biophys Acta. 2006; 1762:1051–1067. [PubMed: 16713195]

Boillée S, Vande Velde C, Cleveland D. ALS: a disease of motor neurons and their nonneuronal neighbors. Neuron. 2006; 52:39–59. [PubMed: 17015226]

Borchelt DR, Lee MK, Slunt HS, Guarnieri M, Xu ZS, Wong PC, Brown RH, Price DL, Sisodia SS, Cleveland DW. Superoxide dismutase 1 with mutations linked to familial amyotrophic lateral sclerosis possesses significant activity. Proc Natl Acad Sci USA. 1994; 91:8292–8296. [PubMed: 8058797]

Comley LH, Wishart TM, Baxter B, Murray LM, Nimmo A, Thomson D, Parson SH, Gillingwater TH. Induction of cell stress in neurons from transgenic mice expressing yellow fluorescent protein: implications for neurodegeneration research. PLoS ONE. 2011; 6:e17639. [PubMed: 21408118]

Crow JP, Calingasan NY, Chen J, Hill JL, Beal MF. Manganese porphyrin given at symptom onset markedly extends survival of ALS mice. Ann Neurol. 2005; 58:258–265. [PubMed: 16049935]

Desnuelle C, Dib M, Garrel C, Favier A. A double-blind, placebo-controlled randomized clinical trial of alpha-tocopherol (vitamin E) in the treatment of amyotrophic lateral sclerosis. ALS riluzole-tocopherol Study Group. Amyotroph Lateral Scler Other Motor Neuron Disord. 2001; 2:9–18. [PubMed: 11465936]

Elchuri S, Oberley TD, Qi W, Eisenstein RS, Jackson Roberts L, Van Remmen H, Epstein CJ, Huang TT. CuZnSOD deficiency leads to persistent and widespread oxidative damage and hepatocarcinogenesis later in life. Oncogene. 2005; 24:367–380. [PubMed: 15531919]

Fischer LR, Culver D, Tennant P, Davis A, Wang M, Castellano-Sanchez A, Khan J, Polak MA, Glass J. Amyotrophic lateral sclerosis is a distal axonopathy: evidence in mice and man. Exp Neurol. 2004; 185:232–240. [PubMed: 14736504]

Fischer LR, Igoudjil A, Magrané J, Li Y, Hansen JM, Manfredi G, Glass JD. SOD1 targeted to the mitochondrial intermembrane space prevents motor neuropathy in the Sod1 knockout mouse. Brain. 2011; 134:196–209. [PubMed: 21078595]

Flood DG, Reaume AG, Gruner JA, Hoffman EK, Hirsch JD, Lin YG, Dorfman KS, Scott RW. Hindlimb motor neurons require Cu/Zn superoxide dismutase for maintenance of neuromuscular junctions. Am J Pathol. 1999; 155:663–672. [PubMed: 10433959]

Glass J, Griffin JW. Neurofilament redistribution in transected nerves: evidence for bidirectional transport of neurofilaments. J Neurosci. 1991; 11:3146–3154. [PubMed: 1941078]

Graf M, Ecker D, Horowski R, Kramer B, Riederer P, Gerlach M, Hager C, Ludolph AC, Becker G, Osterhage J, Jost WH, Schrank B, Stein C, Kostopulos P, Lubik S, Wekwerth K, Dengler R, Troeger M, Wuerz A, Hoge A, Schrader C, Schimke N, Krampfl K, Petri S, Zierz S, Eger K, Neudecker S, Traufeller K, Sievert M, Neundörfer B, Hecht M, Group GvEAS. High dose vitamin E therapy in amyotrophic lateral sclerosis as add-on therapy to riluzole: results of a placebo-controlled double-blind study. J Neural Transm. 2005; 112:649–660. [PubMed: 15517433]

Harraz MM, Marden JJ, Zhou W, Zhang Y, Williams A, Sharov VS, Nelson K, Luo M, Paulson H, Schöneich C, Engelhardt JF. SOD1 mutations disrupt redox-sensitive Rac regulation of NADPH oxidase in a familial ALS model. J Clin Invest. 2008; 118:659–670. [PubMed: 18219391]

Hegedus J, Putman CT, Gordon T. Time course of preferential motor unit loss in the SOD1 G93A mouse model of amyotrophic lateral sclerosis. Neurobiol Dis. 2007; 28:154–164. [PubMed: 17766128]

Hsieh ST, Chiang HY, Lin WM. Pathology of nerve terminal degeneration in the skin. J Neuropathol Exp Neurol. 2000; 59:297–307. [PubMed: 10759185]

Huang TT, Yasunami M, Carlson EJ, Gillespie AM, Reaume AG, Hoffman EK, Chan PH, Scott RW, Epstein CJ. Superoxide-mediated cytotoxicity in superoxide dismutase-deficient fetal fibroblasts. Arch Biochem Biophys. 1997; 344:424–432. [PubMed: 9264557]

Jones DP. Redox potential of GSH/GSSG couple: assay and biological significance. Meth Enzymol. 2002; 348:93–112. [PubMed: 11885298]

Jones DP. Extracellular redox state: refining the definition of oxidative stress in aging. Rejuvenation Res. 2006; 9:169–181. [PubMed: 16706639]

Jones DP, Go YM, Anderson CL, Ziegler TR, Kinkade JM, Kirlin WG. Cysteine/cystine couple is a newly recognized node in the circuitry for biologic redox signaling and control. FASEB J. 2004; 18:1246–1248. [PubMed: 15180957]

Jones DP, Maellaro E, Jiang S, Slater AF, Orrenius S. Effects of N-acetyl-L-cysteine on T-cell apoptosis are not mediated by increased cellular glutathione. Immunol Lett. 1995; 45:205–209. [PubMed: 7558175]

Louwerse ES, Weverling GJ, Bossuyt PM, Meyjes FE, de Jong JM. Randomized, double-blind, controlled trial of acetylcysteine in amyotrophic lateral sclerosis. Arch Neurol. 1995; 52:559–564. [PubMed: 7763202]

Marden JJ, Harraz MM, Williams AJ, Nelson K, Luo M, Paulson H, Engelhardt JF. Redox modifier genes in amyotrophic lateral sclerosis in mice. J Clin Invest. 2007; 117:2913–2919. [PubMed: 17853944]

Muller F, Song W, Jang Y, Liu Y, Sabia M, Richardson A, Van Remmen H. Denervation-induced skeletal muscle atrophy is associated with increased mitochondrial ROS production. Am J Physiol Regul Integr Comp Physiol. 2007; 293:R1159–R1168. [PubMed: 17584954]

Muller F, Song W, Liu Y, Chaudhuri A, Piekedahl S, Strong R, Huang T, Epstein C, Robertsii L, Csete M. Absence of CuZn superoxide dismutase leads to elevated oxidative stress and acceleration of age-dependent skeletal muscle atrophy. Free Radic Biol Med. 2006; 40:1993–2004. [PubMed: 16716900]

Muller FL, Liu Y, Van Remmen H. Complex III releases superoxide to both sides of the inner mitochondrial membrane. J Biol Chem. 2004; 279:49064–49073. [PubMed: 15317809]

Murray LM, Comley LH, Thomson D, Parkinson N, Talbot K, Gillingwater T. Selective vulnerability of motor neurons and dissociation of pre- and post-synaptic pathology at the neuromuscular junction in mouse models of spinal muscular atrophy. Hum Mol Genet. 2008; 17:949–962. [PubMed: 18065780]

Pun S, Santos AF, Saxena S, Xu L, Caroni P. Selective vulnerability and pruning of phasic motoneuron axons in motoneuron disease alleviated by CNTF. Nat Neurosci. 2006; 9:408–419. [PubMed: 16474388]

Reaume AG, Elliott JL, Hoffman EK, Kowall NW, Ferrante RJ, Siwek DF, Wilcox HM, Flood DG, Beal MF, Brown RH, Scott RW, Snider WD. Motor neurons in Cu/Zn superoxide dismutase-deficient mice develop normally but exhibit enhanced cell death after axonal injury. Nat Genet. 1996; 13:43–47. [PubMed: 8673102]

Rothstein J. Current hypotheses for the underlying biology of amyotrophic lateral sclerosis. Ann Neurol. 2009; 65(Suppl 1):S3–9. [PubMed: 19191304]

Schafer FQ, Buettner GR. Redox environment of the cell as viewed through the redox state of the glutathione disulfide/glutathione couple. Free Radic Biol Med. 2001; 30:1191–1212. [PubMed: 11368918]

Shefner JM, Reaume AG, Flood DG, Scott RW, Kowall NW, Ferrante RJ, Siwek DF, Upton-Rice M, Brown RH. Mice lacking cytosolic copper/zinc superoxide dismutase display a distinctive motor axonopathy. Neurology. 1999; 53:1239–1246. [PubMed: 10522879]

Tam SL, Gordon T. Mechanisms controlling axonal sprouting at the neuromuscular junction. J Neurocytol. 2003; 32:961–974. [PubMed: 15034279]

Turner B, Lopes E, Cheema S. Neuromuscular accumulation of mutant superoxide dismutase 1 aggregates in a transgenic mouse model of familial amyotrophic lateral sclerosis. Neurosci Lett. 2003; 350:132–136. [PubMed: 12972170]

Vijayvergiya C, Beal MF, Buck J, Manfredi G. Mutant superoxide dismutase 1 forms aggregates in the brain mitochondrial matrix of amyotrophic lateral sclerosis mice. J Neurosci. 2005; 25:2463–2470. [PubMed: 15758154]

Weisiger RA, Fridovich I. Mitochondrial superoxide dismutase. Site of synthesis and intramitochondrial localization. J Biol Chem. 1973; 248:4793–4796. [PubMed: 4578091]

Wigston DJ, English AW. Fiber-type proportions in mammalian soleus muscle during postnatal development. J Neurobiol. 1992; 23:61–70. [PubMed: 1564455]

Highlights

SOD1 knockout mice develop an oxidative stress-mediated motor axonopathy.

Fast twitch muscle is preferentially denervated.

Motor axon terminals show abnormal sprouting and axon swelling.

Peripheral nerve, not muscle, shows an abnormal GSH redox potential.

N-acetylcysteine rescues axon outgrowth in SOD1 knockout primary motor neurons.

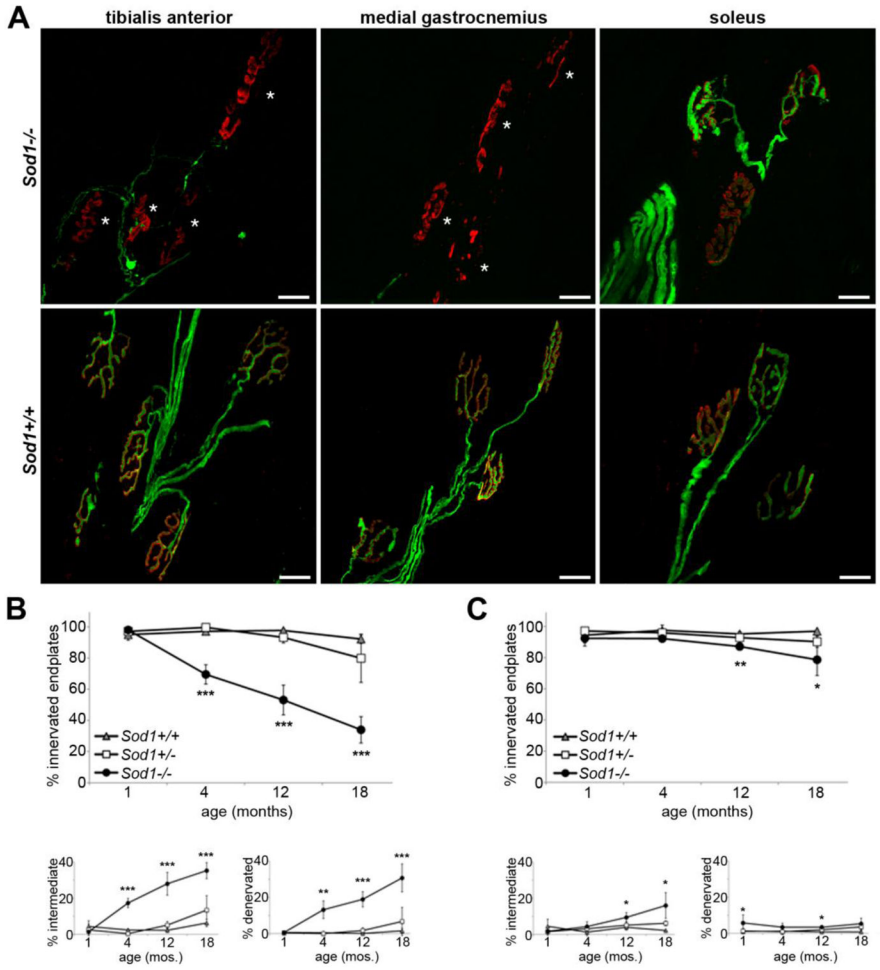

Figure 1.

Denervation in *Sod1−/−* hind limb muscles preferentially affects fast twitch muscles. **A.** Representative confocal projections of tibialis anterior (fast twitch), medial gastrocnemius (fast twitch), and soleus (slow twitch) from 18 month-old *Sod1−/−* mice and *Sod1+/+* littermates, with motor axons in green (YFP) and endplates in red (bungarotoxin). Tibialis anterior and medial gastrocnemius muscles have undergone extensive denervation, but the majority of neuromuscular junctions in soleus remain innervated. **B.–C.** Percent innervated, intermediate, and denervated endplates in tibialis anterior (**B**) and soleus muscle (**C**) from 1 to 18 months of age. Denervation in the soleus muscle is milder than in TA and does not begin until 12 months of age *(n=3–7 animals per group, *p<0.05, **p<0.01, ***p<0.001 vs. Sod1+/+).*

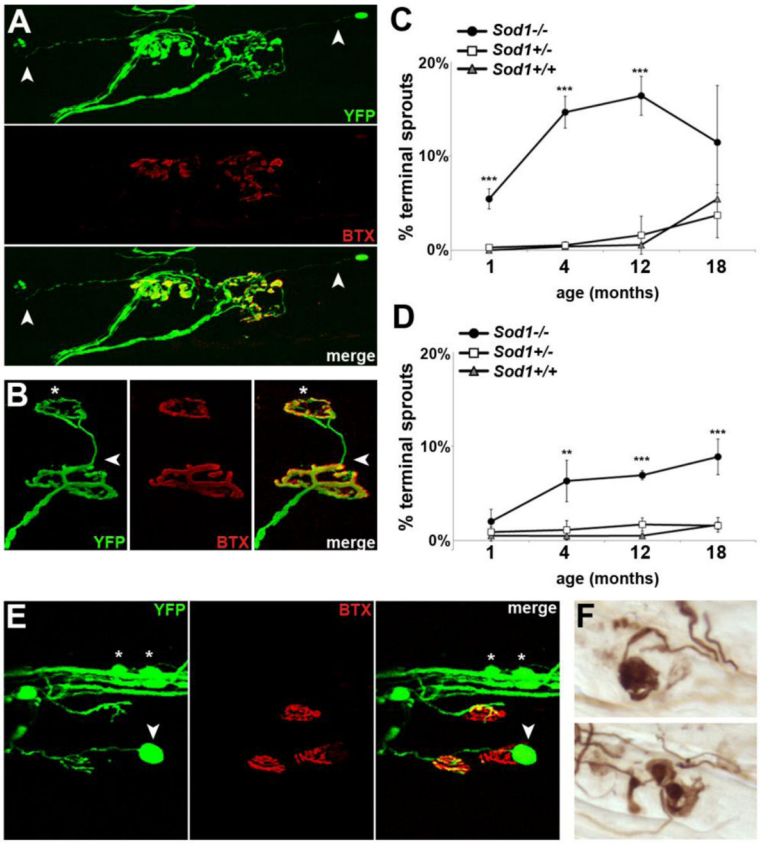

Figure 2.

Loss of SOD1 causes morphologic abnormalities at the neuromuscular junction. **A.** Long terminal sprouts (arrow) arising from innervated junctions. **B.** A terminal sprout (arrow) that has reinnervated a nearby endplate (*). **C.** Percent of endplates in TA showing terminal sprouts. By 1 month of age, prior to the onset of denervation, a significant percent of NMJs already show sprouting. **D.** Percent of endplates in soleus muscle with terminal sprouts. Again, significant sprouting is seen by 4 months, in advance of denervation (In **C–D,** *n=3–7 animals per group; **p<0.01, ***p<0.001 vs. Sod1+/+ and +/−*). **E.** A terminal axon swellings (arrow), along with smaller varicosities involving the intramuscular nerve bundle (*). **F.** Terminal axon swellings show dense accumulation of phosphorylated neurofilament (SMI-31). All images in A–F from *Sod1−/−* tibialis anterior, 4 months of age.

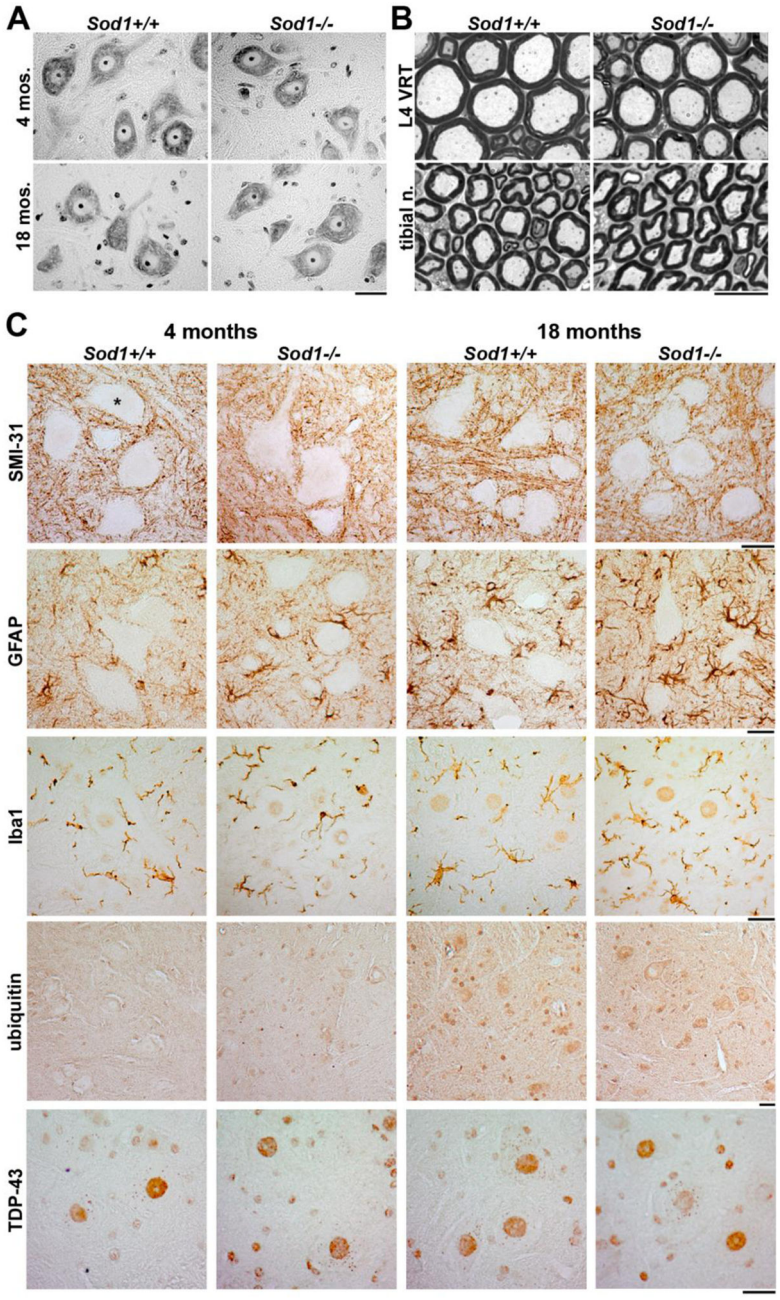

Figure 3.

Sod1−/− mice lack pathologic involvement of lumbar spinal cord and proximal axons. **A.** Morphology of Nissl-stained motor neurons in *Sod1−/−* lumbar spinal cord is identical to wild type at 4 and 18 months of age (*scale bar = 25 μm*). **B.** No degenerating axons are seen in *Sod1−/−* L4 ventral root and tibial nerve at 18 months of age (*scale bar = 10 μm*). **C.** Immunohistochemical staining shows little evidence for pathologic involvement of *Sod1−/−* lumbar spinal cord (representative ventral horns are shown from n=3 mice examined at each stage; motor neuron cell bodies are not counterstained in these sections). Phosphorylated NF-H/NF-M does not accumulate in motor neuron cell bodies (*) or proximal axons

(SMI-31). A mild increase in GFAP-positive astrocytes in *Sod1*−/− mice is seen at both 4 and 18 months of age, but no apparent microgliosis (Iba1). No ubiquitin- or TDP-43-positive inclusions are present, and nuclear TDP-43 localization appears similar in *Sod1*−/− mice and controls (*scale bars = 25 μm*).

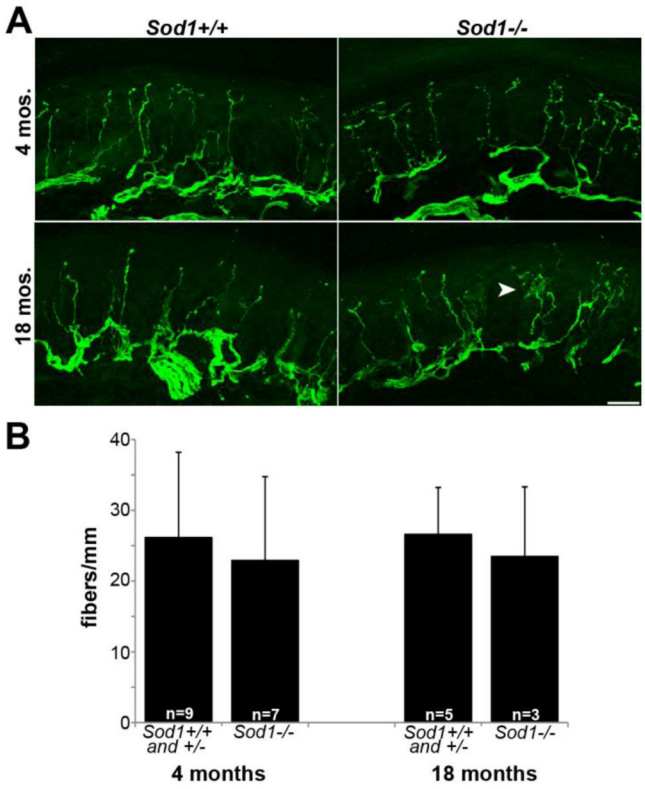

Figure 4.

Distal sensory fibers do not degenerate in *Sod1−/−* mice. **A.** PGP9.5-labelled epidermal nerve fibers from the plantar footpad of *Sod1−/−* mice remain intact at 4 and 18 months of age. A subtle increase in intra-epidermal branching (arrow) is present in 18 month-old *Sod1−/−* mice (*scale bar = 20 μm*). **B.** Epidermal nerve fiber density, expressed as the number of fibers/mm of epidermis, is equivalent in *Sod1−/−* mice and controls (number of animals is indicated on bar graph).

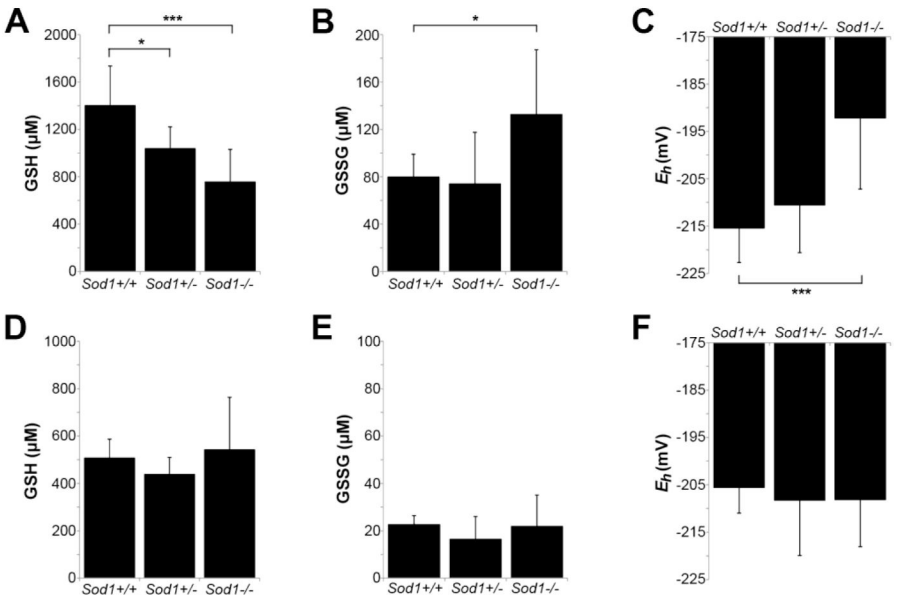

Figure 5.

Loss of SOD1 leads to a more oxidized redox state in peripheral nerve, but not muscle, by 4 months of age. **A–C.** GSH (**A**) and GSSG (**B**) levels from tibial nerve of 4 month-old mice, measured by HPLC, and the calculated redox potential (E_h) (**C**). *Eh* is approximately 20 mV higher (more oxidized) in tibial nerve of 4 month-old *Sod1*−/− mice compared to controls (*$p<0.05$, ***$p<0.001$). **D–F.** GSH (**D**), GSSG (**E**), and E_h (**F**) from gastrocnemius muscle show no difference between *Sod1*−/− and controls (same animals as in A–C). For all panels, n=7 (*Sod1*+/+), n=13 (*Sod1*+/−), n=14 (*Sod1*−/−).

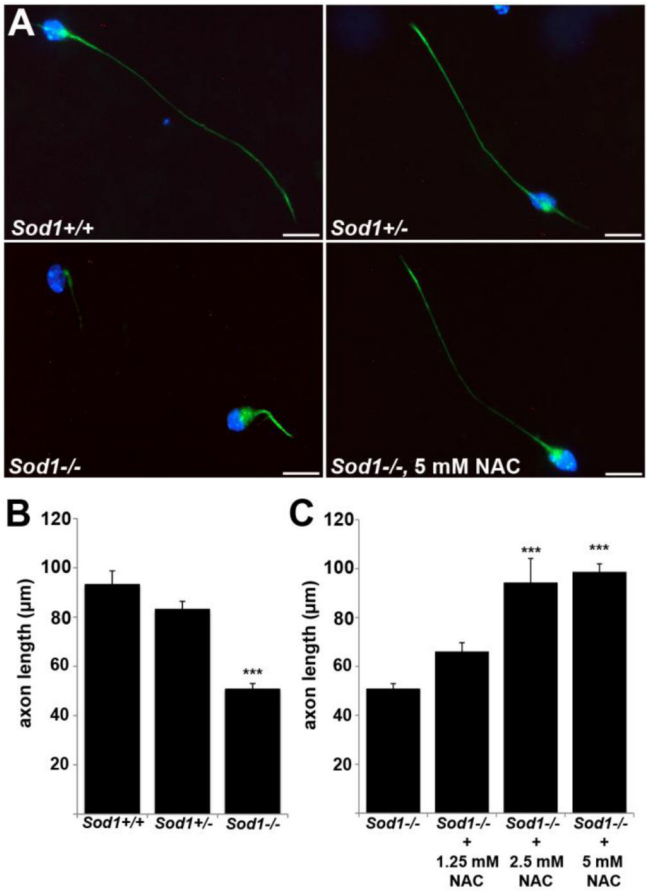

Figure 6.

Poor axon outgrowth in *Sod1−/−* primary motor neurons is rescued by antioxidant treatment. **A.** Primary motor neurons at 24 hrs in culture, labeled with phosphorylated neurofilament (green) and DAPI (blue). *Sod1−/−* motor neurons show significantly shorter axons than *Sod1+/+* and *Sod1+/−* neurons at 24 hrs. Treatment with 5 mM NAC restores *Sod1−/−* axons to wild-type length (*scale bar = 20 µm*). **B.–C.** Mean axon length at 24 hrs ± SEM from 4 independent experiments is shown. 500–600 neurons per group were measured *(***p<0.001 vs. Sod1+/+ and +/− (B); or vs. Sod1−/− (C)).*